

Influence of $\text{Fe}^{3+}/\text{Fe}^{2+}$ Ratio on the Crystallization of Iron-Rich Glasses Made with Industrial Wastes

Alexander Karamanov, Paola Piscicella, Carlo Cantalini, and Mario Pelino*

Department of Chemistry, Chemical Engineering, and Materials, University of L'Aquila, L'Aquila, Italy

The influence of the $\text{Fe}^{3+}/\text{Fe}^{2+}$ ratio on the crystallization of iron-rich glasses was investigated in this study. The glass batches were made from two hazardous industrial wastes: mud (goethite and jarosite) originating from the zinc hydrometallurgical process and electric arc furnace dust (EAFD). Glass compositions were prepared by adding different percentages of carbon powder. The crystallization process was investigated by a combined thermogravimetry/differential thermal analysis technique, in air or nitrogen atmospheres, using powder and bulk glass samples. The crystalline phases formed, i.e., pyroxene and spinels, and their relative ratio were determined by X-ray diffractometry. The experimental results indicated that melting temperature and crystallization behavior were influenced by the initial $\text{Fe}^{3+}/\text{Fe}^{2+}$ ratio and by the amount of carbon added to the glass batch. For goethite and jarosite glass compositions, decreasing the $\text{Fe}^{3+}/\text{Fe}^{2+}$ ratio increased the crystallization rate by favoring magnetite formation. For EAFD glass compositions, the addition of carbon to the batch inhibited chromite–magnetite spinel formation and favored the attainment of an amorphous glassy phase.

I. Introduction

IRON is one of the elements present in great quantity in natural volcanic rocks; some basalts contain as much as 10–15 wt% iron oxides.¹ The iron-rich glass-forming compositions are well known and widely used in the petrological industry for the production of glass fibers and glass-ceramic tile by melting, fibering, or casting–rolling natural basalt rocks.^{2–5} Petrological products are characterized by high abrasion and corrosion resistance and high mechanical strength.

Iron-rich silicate and borosilicate glass compositions are used for nuclear waste disposal.^{6–10} Vitrification atomistically bonds the radioactive elements in a chemically stable glass network and provides an exceptional volume reduction. When secondary crystallization improves the chemical durability of the glass, crystallization heat treatment can also occur.^{11–13}

Recently, high-iron-content glasses, up to 30% Fe_2O_3 , have been widely investigated, because the vitrification of hazardous wastes, mainly industrial mud or ashes from metallurgical processes, is becoming an environmentally accepted means to stabilize regulated heavy metals.^{14–23}

Iron-rich glass compositions have a high driving force to crystallize, and an amorphous structure is often obtained only after quenching in water (glass frit).^{14,15} These compositions are characterized by a tendency to undergo liquid immiscibility. One of the liquid phases is richer in iron and promotes formation of the

magnetite spinel as the first crystal phase.^{3,4,16,18,23} When a high percentage of Cr_2O_3 is present in the composition, such as in electric arc furnace dust (EAFD) containing glasses,²² the crystallization rate increases because of the low solubility of Cr_2O_3 in silicate melts and the rapid formation of Cr-Fe spinels. The spinels have a simple cubic unit cell, corresponding to the general formula $\text{M}_8^{2+}\text{M}_{16}^{3+}\text{O}_{32}$ ($\text{M}^{2+}\text{M}_2^{3+}\text{O}_4$). This mineralogical group may be subdivided into three series, according to the nature of the M^{3+} ion: Al (spinel series), Fe^{3+} (magnetite series), and Cr (chromite series).²⁴ The M^{2+} positions may be occupied by Mg^{2+} , Fe^{2+} , Zn^{2+} , Mn^{2+} , and other two-valence cations with small radii. All spinels easily form solid solutions.

With prolonged thermal treatment, a monoclinic pyroxene solid solution precipitates onto the spinel crystals, which act as nuclei for crystallization.^{3,4,13,14,18,23} The monoclinic pyroxenes ($\text{M}^*\text{M}^{**}\text{SiO}_6$) are the chain silicates with the simplest structure, made up of silicon-oxygen tetrahedra bonded at two corners and forming infinite chains (SiO_3)²⁻. These chains are linked by octahedral layers containing 6–8 coordinated cations, generally Mg, Ca, and Fe^{2+} , or, eventually, Fe^{3+} , together with Na.²⁴

In the iron-rich glasses, the iron can exist in either the ferrous or the ferric oxidation state. In the amorphous structure, the Fe^{3+} can be considered an intermediate ion, whereas the Fe^{2+} is typically a modifying ion.^{25,26} The $\text{Fe}^{3+}/\text{Fe}^{2+}$ ratio in a glass generally depends on the chemical compositions and melting conditions,^{10,26} which are controlled by the presence of oxidizing or reducing agents in the batch.^{3,20} The $\text{Fe}^{3+}/\text{Fe}^{2+}$ ratio influences the viscosity curve and liquidus temperature: i.e., the lower the ratio, the lower the viscosity and the liquidus temperature.^{19,25} The crystallization rate, spinel/pyroxene ratio, and final properties of the glass-ceramic are also influenced by the $\text{Fe}^{3+}/\text{Fe}^{2+}$ ratio.

The present study was aimed at investigating the influence of the $\text{Fe}^{3+}/\text{Fe}^{2+}$ ratio on the crystallization of iron-rich glasses obtained from two hazardous industrial wastes, mud arising from the zinc hydrometallurgical process and EAFD.

II. Experimental Procedure

The wastes investigated in the present study included goethite and jarosite, which are present in the iron-rich hazardous mud coming from the hydrometallurgical process used in the production of zinc metal.¹⁴ The present samples were obtained from zinc plants located in Sardinia, Italy, and in Asturias, Spain. Electric-arc-furnace baghouse dust is a waste byproduct from the steelmaking process; it contains the elements that are volatilized from the charge during melting. The sample investigated was obtained from a stainless-steel plant located in northern Italy.¹⁹

Chemical analyses of the wastes were conducted using an energy dispersive X-ray (EDX) radio-frequency instrument (Xepos, Spectro Analytical Instruments, GmbH, Kleve, Germany) equipped with a 50 W rhodium anode X-ray tube. The results, expressed as wt% of the oxides, are shown in Table I.

Different batch compositions were prepared by mixing the wastes in various proportions with glass cullet, sand, limestone, and soda. Fine carbon powder was added in different percentages

C. M. Jantzen—contributing editor

Manuscript No. 188839. Received January 3, 2000; approved June 30, 2000.
*Member, American Ceramic Society.

Table I. Chemical Compositions of the Industrial Wastes and Investigated Glasses Used in the Present Study[†]

	Goethite	Jarosite	EAFD	Glass "G"	Glass "J"	Glass "D"
SiO ₂	2.2	3.7	5.1	45.6	55.3	39.2
TiO ₂				2.0		
Al ₂ O ₃	0.7	0.3	1.2	3.3	3.8	1.0
Fe ₂ O ₃	51.3	49.2	21.1	25.5	22.8	10.9
Cr ₂ O ₃			20.5			10.3
MgO		0.2	17.0	1.6	0.2	11
CaO	0.1	0.1	10.5	4.5	6.9	9.3
PbO	6.3	4.0	0.4	3.1	1.6	0.2
ZnO	13.3	5.6	3.8	6.5	2.5	1.9
MnO			9.3			4.7
CdO	0.4			0.2		
NiO	0.4		3.7	0.2		1.8
CuO	0.5			0.3		
Na ₂ O	0.1	0.1	2.9	6.2	5.9	7.6
K ₂ O			3.2	1.0	1.0	2.1
LOI [‡]	24.7	36.9	1.6			

[†]All values are in wt%. [‡]Loss on ignition.

to some batch compositions, to provide reducing conditions. The melting behavior was investigated by thermogravimetry/differential thermal analysis (TG-DTA).

Glasses were melted at 1400°–1550°C in a super kanthal electric furnace, using 100 mL corundum crucibles (99.8% Al₂O₃). Part of the melt was quenched in a stainless-steel mold and part in water, to obtain a glass frit. The as-made compositions used in the present study are also summarized in Table I. The iron is presented as Fe₂O₃.

After annealing of the glass, the Fe³⁺/Fe²⁺ ratio was evaluated by the spectrophotometric method. The crystallization process was investigated under nonisothermal conditions, by means of the TG + DTA technique, at a 10°C/min heating rate. Powder samples (~100 mg, <300 μm) obtained after crushing and sieving the glass frit were thermally treated in the 20°–1000°C range, in air or nitrogen atmospheres. TG-DTA analyses were also conducted on bulk glass samples in air.

The crystalline phases formed were determined by X-ray diffractometry (XRD; Model No. 1830, Philips Electronic Instruments, Almelo, The Netherlands), using CuKα radiation. The crystalline fractions were evaluated by comparing the areas of peaks for the amorphous and crystalline phases in the XRD spectra.²⁷ The ratio between the amounts of the crystalline phases was estimated using the relative intensities of the major peaks.²⁸

III. Results and Discussion

(I) Goethite and Jarosite Glasses

In goethite and jarosite wastes, the iron is in the ferric state, and the Fe³⁺/Fe²⁺ ratio is not modified by melting; therefore, to increase the Fe²⁺ percentage, carbon powder was used as a reducing agent in the batch.

Figure 1 shows the result for the Fe³⁺/Fe²⁺ ratio in the goethite glass, labeled "G," as a function of the percentage of carbon powder in the batch.¹² In these experiments, the melting temperature and time were 1450°C and 3 h, respectively. The Fe³⁺/Fe²⁺ stoichiometric ratio for magnetite (which is 2.0) was obtained with ~1.5% carbon. Similar results were obtained for jarosite glasses. Two batches, one with no carbon (J-0) and one with 2% carbon (J-2) were melted for 2 h at 1450°C. The Fe³⁺/Fe²⁺ ratios in the glasses were ~10.5 for J-0 and 2.1 for J-2. The crystallization process was investigated by TG-DTA conducted on powder and bulk glass samples. The TG-DTA traces for the J-0 and J-2 samples are shown in Figs. 2 and 3, respectively. The DTA (solid line) and the TG (broken line) plots are reported for the powder samples heat-treated in air and nitrogen atmospheres (P-air and P-N₂, respectively) and for the bulk sample heat-treated in air (B-air).

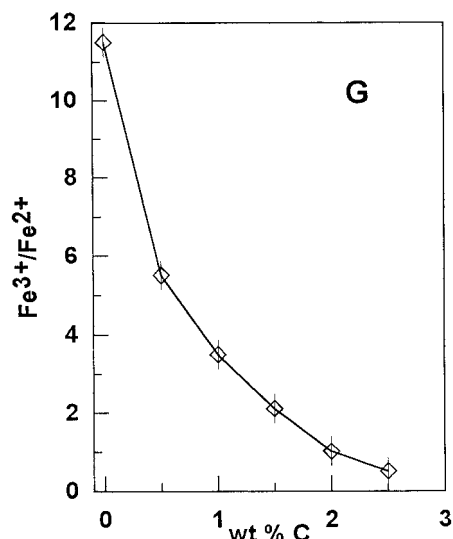


Fig. 1. Fe³⁺/Fe²⁺ ratio in goethite ("G") glass, as a function of the percentage of carbon powder in the batch.

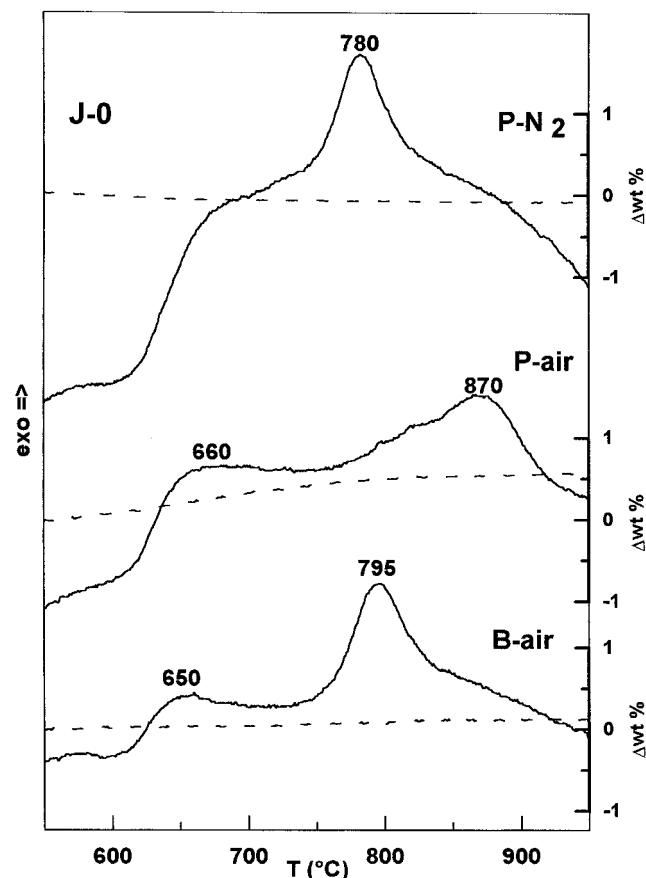


Fig. 2. TG (---) and DTA (—) plots of J-0 composition: powder samples heat-treated in air (P-air) and nitrogen (P-N₂); bulk sample heat-treated in air (B-air).

For J-0 glass, the TG trace of P-air shows a detectable increase in weight, ~0.5%, after 600°C, attributed to the oxidation process of Fe²⁺ to yield Fe³⁺. This weight change is connected with an exothermic effect, having its maximum at 660°C. The crystallization peak in the same graph occurs at 870°C. When the powder J-0 sample is heat-treated in N₂ (P-N₂), no TG variation is detected, and the only exothermic peak is relative to the crystallization. Here, the peak temperature is lower (780°C), indicating a more

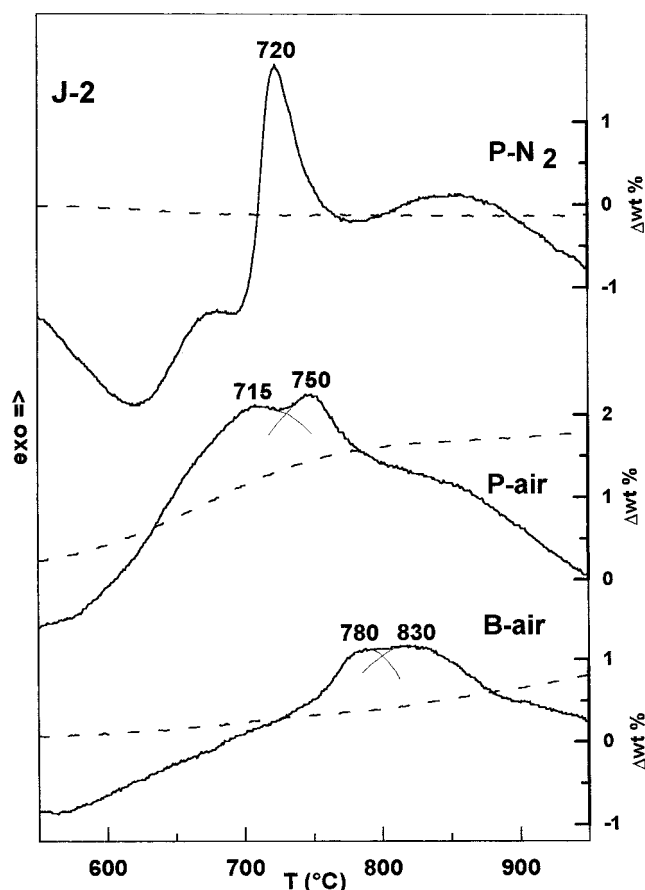


Fig. 3. TG (---) and DTA (—) plots of J-2 composition: powder samples heat-treated in air (P-air) and nitrogen (P-N₂); bulk sample heat-treated in air (B-air).

rapid crystallization process. Finally, when the J-0 bulk sample is heat-treated in air (B-air), no weight variation appears in the TG trace; the oxidation exopeak is negligible, and the crystallization exopeak occurs at 795°C.

A previous paper¹⁹ reported that, for jarosite glass made without carbon addition in the batch, the crystallization of glass powder in air was inhibited by the surface oxidation of Fe^{2+} . In fact, oxidation influences the rate of crystal growth by increasing the viscosity and liquidus temperature. The oxidation of powdered iron-rich glasses also leads to a decrease in the total amount of crystal phase formed and changes the reaction order of the crystallization process.²³

For J-2 glass, the oxidation of Fe^{2+} to yield Fe^{3+} is more evident, because of the higher Fe^{2+} content. The weight gains are ~2% for P-air and ~1% for B-air samples. In J-2 glass, the crystallization and oxidation processes occur simultaneously, and the two peaks overlap in the DTA trace. The oxidation exopeak has a maximum at ~715°C for P-air and 830°C for B-air samples. These temperatures correspond to the middle of the increasing of the TG trace. The differences of peak temperature and weight gain between the two samples occur because oxidation is controlled by the diffusion of the Fe^{2+} ions from the bulk to the surface¹⁹ and, therefore, is more rapid in the powder sample. The crystallization peaks have maxima at 780°, 750°, and 720°C for the B-air, P-air, and P-N₂ samples, respectively. This result highlights that the crystallization process always occurs at a lower temperature in J-2 samples than in J-0 samples, an indication of a higher crystallization rate in the J-2 samples.

XRD analyses of powder and bulk samples of J-0 and J-2 glasses were made after 1 h heat treatment at 900°C, conditions corresponding to completion of crystallization. Table II reports the weight percentage of crystal phase formed in each sample and the

Table II. Percentages of Crystal Phases Formed and Magnetite/Pyroxene Ratios[†]

	J-0		J-2	
	Powder	Bulk	Powder	Bulk
Crystal phase (wt%)	42 ± 2	52 ± 2	38 ± 2	46 ± 2
M/P ratio [‡]	38/100	45/100	100/85	90/100
Magnetite (wt%)	11 ± 2	15 ± 2	20 ± 2	22 ± 2
Pyroxene (wt%)	31 ± 2	37 ± 2	18 ± 2	24 ± 2

[†]Powder and bulk J-0 and J-2 samples after 1 h heat treatment at 900°C.
[‡]M—magnetite; P—pyroxene.

relative magnetite/pyroxene ratio. A comparison of the XRD spectra reveals that, in the both compositions, the amount of crystal phase is lower in the P samples than in the B samples because of less magnetite formation induced by the surface oxidation. As a result, pyroxene formation is also negatively influenced, because this crystalline phase precipitates by reaction of the glass with the magnetite crystals and because oxidation also leads to the migration of the iron from the bulk to the surface layer, so that fewer Fe^{2+} ions are available to enter into the pyroxene structure. At higher temperatures (950°–1000°C), hematite (Fe_2O_3) forms on the iron-enriched surface layer.^{16,19}

In J-2 samples, the magnetite/pyroxene ratio is considerably higher than in J-0 samples, because of the lower initial Fe^{3+}/Fe^{2+} ratio; less magnetite phase is also observed in the powder J-2 samples than in the corresponding B samples. Therefore, the addition of 1.5%–2.0% carbon to the batch increases the amount of magnetite phase and, as a result, enhances the crystallization rate. However, this result is connected with a decrease in the total amount of crystal phase, because of the formation of less pyroxene phase.

Carbon addition also influences the melting process, by decreasing both the viscosity and liquidus temperatures.^{25,26} The DTA results of the J-0 and J-2 batches show this effect, in that the melting effect for the J-2 batch starts at ~940°C, whereas the same effect for the J-0 starts at 1060°C.

(2) EAFD Glasses

The EAFD glass, labeled “D,” was prepared by mixing 50 parts of EAFD with 50 parts of container-glass cullet. Three compositions were melted: one with no carbon (D-0), and two others with 2% and 5% carbon in the batch (D-2 and D-5, respectively).

Because of the spontaneous crystallization of the melt in the crucible, quenching of the D-0 composition was impossible, even after an increase in the melting temperature up to 1600°C. Samples D-2 and D-5 were quenched in the stainless-steel mold and in water, after being melted for 1 h at 1550° and 1500°C, respectively. Values of 9.1 and 0.2 were obtained for the Fe^{3+}/Fe^{2+} ratios of the D-0 and D-5, respectively.

After the D-0 was cooled, the total amount of crystalline phase was evaluated as 72% ± 2%, with a spinel/pyroxene relative ratio of ~100/45. The XRD spectrum is reported in Fig. 4(a).

The quenching of sample D-2 into the metal mold also yielded a crystalline XRD spectrum, but with a lower degree of crystallization than that of the D-0. The quenching of D-2 in water yielded a crystal spinel phase of 26% ± 2%.

After quenching into the metallic mold, the XRD spectrum of sample D-5 showed only the major peaks of the chromite spinels, corresponding to ~15 ± 2 wt%. In fact, Cr_2O_3 in concentrations >1% is insoluble in the silicate melt and precipitates as isolated nuclei in the amorphous matrix. The spectrum of the D-5 sample is shown in Fig. 4(b).

The D-5 sample was subjected to thermal treatment at 20°C/min by TG-DTA. The DTA trace, reported in Fig. 5, shows a glass-transition temperature, T_g , at ~610°C and a crystallization peak at 765°C. The exothermic peak is particularly sharp and intense and is close to T_g , an indication of a high crystallization rate. A weight gain of ~2% is evident in the TG curve, resulting

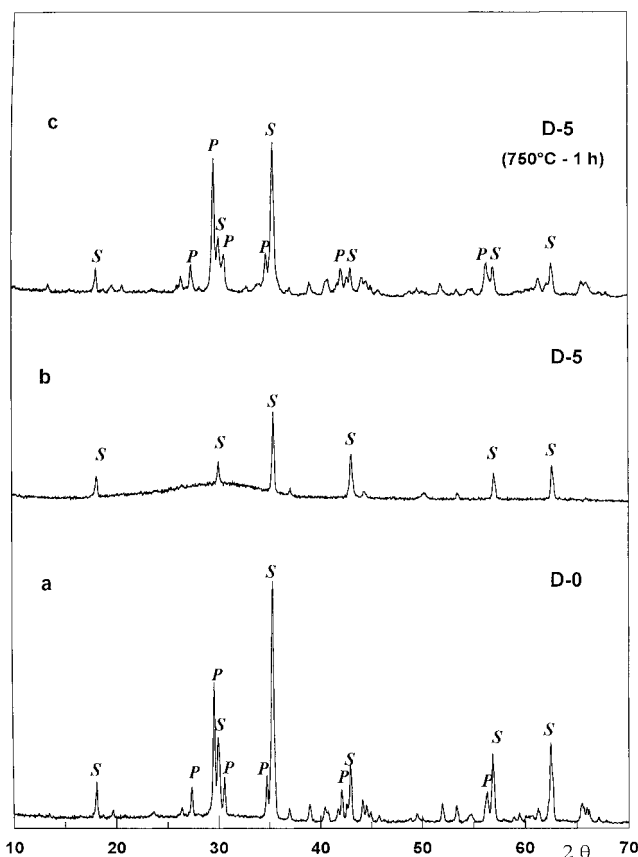


Fig. 4. XRD spectra of bulk D-0 and D-5 samples: (a) D-0 after quenching in air; (b) D-5 after quenching in air; (c) D-0 after 1 h at 750°C ("P" is pyroxene, "S" spinel).

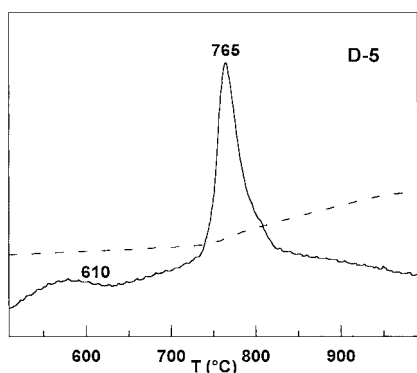


Fig. 5. TG (---) and DTA (—) traces of D-5 bulk sample in air.

from the surface reoxidation of FeO. The XRD spectrum of D-5 after 1 h heat treatment at 750°C is shown in Fig. 4(c). The crystal phase corresponds to $\sim 62\% \pm 2\%$, and the spinel/pyroxene ratio is $\sim 100/80$. Compared with the D-0 sample, the D-5 sample exhibits a consistent decreasing of the spinel phase, whereas the percentage of pyroxene is similar.

The results obtained for the "D" compositions indicate that adding carbon to the glass batch decreases the rate of chromite-magnetite spinel formation. For EAFD glass, the crystallization rate and spinel formation could be assumed to depend on the ratio M^{3+}/M^{2+} , where M^{3+} is the sum ($Cr^{3+} + Fe^{3+}$) and M^{2+} the sum ($Mg + Mn + Zn + Fe^{2+}$). The initial M^{3+}/M^{2+} value for the D-0 composition is 0.71, because of the high molar percentage of MgO and MnO in the glass batch. The addition of carbon decreases this value to 0.27 for the D-5 composition. In practical terms, the amount of spinel and its rate of formation depend on the

($Cr_2O_3 + Fe_2O_3$) mol%. The lower the value of the sum, the lower the percentages of crystal phase formed and the trend of spontaneous crystallization.

IV. Conclusions

The results of the present study highlight the complex role played by the oxidation state of iron in waste-glass compositions made with high iron contents. The melting and crystallization behaviors are influenced by the initial Fe^{3+}/Fe^{2+} ratio and by the addition of carbon to the glass batch.

For the investigated goethite and jarosite compositions, a magnetite ratio of 2 can be obtained by 1.5%–2% carbon addition. Decreasing the Fe^{3+}/Fe^{2+} ratio increases the magnetite formation and the crystallization rate. The magnetite/pyroxene ratio is also increased.

For EAFD compositions, adding carbon to the batch inhibits chromite-magnetite formation. This result reduces the trend to spontaneous crystallization and favors the attainment of an amorphous glassy phase.

Acknowledgments

The authors are grateful to the CNR, under the project, "Materiali Speciali per Tecnologie Avanzate II," for the financial support given to this work. The authors are grateful to Dr. G. Taglieri, Ing S. Crisucci, and Mrs. F. Ferrante for the experimental work.

References

- ¹S. A. Morse, *Basalts and Phase Diagrams*. Springer-Verlag, New York, Heidelberg, Berlin, 1982.
- ²B. Locsei, *Molten Silicates and Their Properties*. Akademiai Kiado, Budapest, Hungary, 1970.
- ³H. Beall and H. L. Rittler, "Basalt Glass Ceramics," *Am. Ceram. Soc. Bull.*, **55** [6] 579–82 (1976).
- ⁴V. Znidarsic-Pongarac and D. Kolar, "The Crystallization of Diabase Glass," *J. Mater. Sci.*, **26**, 2490–94 (1991).
- ⁵J. M. Caceres, J. E. Hernandez, and J. M. Rincon, "Characterization of Fibers as Rockwool for Insulation Obtained from Canary Island Basalts," *Materials Construction*, **46** [242–43] 64–78 (1996).
- ⁶J. M. Welch, R. L. Miller, and J. E. Flinn, "Immobilization of Three-Mile Island Core Debris"; pp. 611–18 in *Advances in Ceramics*, Vol. 8, *Nuclear Waste Management*. Edited by G. G. Wicks and W. A. Ross. American Ceramic Society, Columbus, OH, 1984.
- ⁷C. M. Jantzen, "TTT Kinetics in SRL Waste Glass"; see Ref. 6, pp. 30–38.
- ⁸D. F. Bickford and C. M. Jantzen, "Devitrification of Defense Nuclear Waste Glass: Role of Melt Insolubles," *J. Non-Cryst. Solids*, **84**, 299–307 (1986).
- ⁹R. Richards and M. Plodinec, "Overview of Current and Emerging Waste Vitrification Technologies"; in *Proceedings of the XVIIIth International Congress on Glass (ICG)*. Sect. A7 (San Francisco, CA, July 5–8, 1998). American Ceramic Society, Westerville, OH.
- ¹⁰D. Schreiber, B. K. Kochanowski, and C. W. Shreberg, "Compositional Effect on the Iron Redox State in Model Glasses for Nuclear Waste Immobilization"; pp. 141–50 in *Ceramic Transactions*, Vol. 39, *Environmental and Waste Management Issues in the Ceramic Industry*. Edited by G. B. Mellinger. American Ceramic Society, Westerville, OH, 1994.
- ¹¹D. Kim, P. Hrma, D. Smith, and M. Schweiger, "Crystallization in Simulated Glasses from Hanford High-Level Nuclear Waste Composition Range"; see Ref. 10, pp. 179–89.
- ¹²L. A. Chick, R. O. Lokken, and L. E. Thomas, "Basalt-Glass Ceramics for the Immobilization of Transuranic Nuclear Waste," *Am. Ceram. Soc. Bull.*, **62** [4] 505–10 (1983).
- ¹³E. De Grave, A. D. Stalious, and A. Van Alboom, "Influence of Heat Treatment on the Mossbauer Spectrum of a Simulated Nuclear-Waste Glass," *J. Nucl. Mater.*, **171**, 189–97 (1990).
- ¹⁴M. Pelino, C. Cantalini, C. Abbruzzese, and P. Plescia, "Treatment and Recycling of Goethite Waste Arising from the Hydrometallurgy of Zinc," *Hydrometallurgy*, **40**, 2087–94 (1996).
- ¹⁵M. Pelino, C. Cantalini, and J. M. Rincon, "Preparation and Properties of Glass-Ceramic Materials Obtained by Recycling Goethite Industrial Waste," *J. Mater. Sci.*, **32**, 4655–60 (1997).
- ¹⁶J. M. Rincon, M. Pelino, and M. Romero, "Glass-Ceramics Obtained from Axial Pressing and Sintering of Vitrified High Iron Content Red Mud"; pp. 169–81 in *Valorization and Recycling of Industrial Wastes*, Proceedings of the First National Congress (L'Aquila, Italy, July 7–10, 1997). Mucchi, Modena, Italy.
- ¹⁷M. Pelino, "Recycling of Jarosite Waste in the Production of Glass and Glass-Ceramics Materials," *Interceram.*, **47** [1] 22–26 (1998).

¹⁸A. Karamanov, C. Cantalini, M. Pelino, and A. Hreglich, "Kinetics of Phase Formation in Jarosite Glass-Ceramics," *J. Eur. Ceram. Soc.*, **19** [4] 527–33 (1999).

¹⁹A. Karamanov, G. Taglieri, and M. Pelino, "Iron-Rich Sintered Glass-Ceramics from Industrial Wastes," *J. Am. Ceram. Soc.*, **82** [11] 3012–16 (1999).

²⁰E. Kuleva, L. A. Orlova, O. N. Borisov, and M. Gulikin, "Glass-Ceramics on Base of Iron-Containing Industrial Wastes"; see Ref. 9, Sect. B8.

²¹D. Zunkel, "Electric Arc Furnace Dust Management: A Review of Technologies," *Iron Steel Eng.*, **3**, 135–42 (1997).

²²S. Crisucci, A. Karamanov, P. Pisciella, and M. Pelino, "Stabilization of Electric Arc Furnace Dust (EAFD) by Vitrification Process"; pp. 107–116 in *Valorization and Recycling of Industrial Wastes*, Proceedings of the Second National Congress (L'Aquila, Italy, July 5–8, 1999). Mucchi, Modena, Italy.

²³A. Karamanov, P. Pisciella, and M. Pelino, "The Crystallisation Kinetics of Iron Rich Glass in Different Atmosphere," *J. Eur. Ceram. Soc.*, **20**, 2233–37 (2000).

²⁴W. Deer, R. Howie, and J. Zussman, *An Introduction to the Rock-Forming Minerals*. Longman, Birmingham, AL, 1992.

²⁵W. Eitel, *The Physical Chemistry of the Silicates*. University of Chicago Press, Chicago, IL, 1954.

²⁶A. Appen, *The Chemistry of Glasses* (in Russian). Himiq, Leningrad, U.S.S.R., 1974.

²⁷H. Kim, R. Rawlings, and P. Rogers, "Quantitative Determination of Crystal and Amorphous Phases in Glass-Ceramics by X-ray Diffraction Analysis," *Br. Ceram. Trans. J.*, **88**, 21–25 (1989).

²⁸H. P. Klug and L. E. Alexander, *X-ray Diffraction Procedures for Polycrystalline and Amorphous Materials*. Wiley, New York, 1974. □